AIAA 81-0196R

# Compressible Boundary-Layer Stability Calculations for Sweptback Wings with Suction

Leslie M. Mack*
*Jet Propulsion Laboratory, California Institute of Technology, Pasadena, Calif.*

**The stability of the laminar boundary layers on two transonic wings of infinite span with distributed suction is investigated with the compressible, parallel-flow stability theory. Both wings have supercritical airfoil sections; one has a sweep angle of 23 deg, the other 35 deg. Zero-frequency disturbances are used to represent cross-flow instability, and disturbances with the wavenumber vector aligned with the local flow direction represent traveling-wave instability. In both cases, the maximum spatial amplification rate is used as a measure of the instability. For the suction, distributions with constant mass flux downstream of the starting point are used. The main objective is to determine how the maximum amplification rate varies with the magnitude and starting point of the suction. It is found for both types of disturbances that the maximum amplification rate varies almost linearly with the suction magnitude up to at least the point where the amplification rate is halved. Different starting locations for the suction in the first 4% of the chord were found to affect cross-flow instability, but to have little influence on traveling-wave instability.**

## Introduction

SUCTION is a well-known and much explored method of maintaining laminar boundary-layer flow. In recent years it has become the normal procedure to calculate the suction required to avoid transition to turbulence by means of linear stability theory. This work was started long ago by Brown,[1] and the first application of modern computing methods was by Srokowski and Orszag.[2] A useful review of this subject, together with a comparison of various calculation methods with the available experiments, has been given by Hefner and Bushnell.[3] The stability theory in Refs. 2 and 3 is applied in the form of the $e^n$ method, where $n$ is obtained by integrating a local amplification rate along some specified direction. This method has many difficulties, among them that $n$ at transition can have values ranging from 1 to 20, but it has proven to be useful in engineering studies of laminar flow control systems. A correct computation of the amplitudes of the instability waves produced by specific disturbances in a growing boundary layer is a quite different, and so far, not completely resolved problem.

The $e^n$ method is not used in the present paper as the prediction of whether or not transition will occur, and if so where, is not an objective. Rather, the purpose is to investigate the way in which the local instability responds to systematic changes in the magnitude of the suction. In order to reduce the vast number of calculations that would be needed to carry out this program, the local instability is characterized by the instability of two representative waves. The first of these is the most unstable stationary wave, and represents the cross-flow instability. The second is the most unstable wave with the wavenumber vector aligned with the local flow direction, and represents the traveling-wave, or Tollmien-Schlichting, instability. A further simplification is that of all possible suction distributions, only those where the mass flux is constant along the chord are considered. The chief aim is to determine, by calculation with the compressible, parallel-flow stability theory, whether any simple relationships exist between these two amplification rates and the magnitude of the suction mass flux.

Presented as Paper 81-0196 at the AIAA 19th Aerospace Sciences Meeting, St. Louis, Mo., Jan. 12-15, 1981; submitted Feb. 20, 1981; revision received Aug. 27, 1981. 

*Member of Technical Staff, Molecular Physics and Chemistry Section, Earth and Space Sciences Division. Member AIAA.

This paper is one of a series on the stability of three-dimensional boundary layers. The formulation of the three-dimensional stability theory that is used in the present calculations was first given in Ref. 4; the three-dimensional Falkner-Skan-Cooke incompressible boundary layers were studied in Ref. 5; the compressible stability theory was applied to the same 35 deg transonic swept wing as used here in Ref. 6; and both Falkner-Skan-Cooke boundary layers with suction and the 35 deg swept wing with suction and with surface cooling were studied in Ref. 7. In the present paper, some additional results are given for the 35 deg wing both with constant suction from the leading edge and without suction, but the majority of the results are for a 23 deg swept wing with a radically different pressure distribution. Compressible stability calculations for the 35 deg wing with suction and surface cooling have also been presented by Lekoudis,[8,9] and for the 23 deg wing with suction by El-Hady.[10]

## Mean Flow

The coordinate systems adopted are shown in Fig. 1. The leading edge of the wing forms the $z_s^*$ axis (asterisks refer to dimensional quantities) and the chord the $x_c^*$ axis. The angle of sweep is $\psi_{sw}$. The undisturbed freestream velocity is $U_\infty^*$ and the Mach number $M_\infty$. At a given point along the chord, the local potential velocity is $U_p^*$ with components $U_{ce}^*$ and $W_\infty^*$ in the $x_c^*$ and $z_s^*$ directions, respectively. For the infinite-span wings considered in this paper, $W_\infty^*$ is a constant and equal to its value in the undisturbed freestream. The direction of $U_p^*$ forms the $x^*$ axis of the local coordinate system of the stability analysis. The angle between $U_p^*$ and $U_\infty^*$ is $\psi_p$. The cross flow is in the $z^*$ direction and, by definition, is different from zero only within the boundary layer. The other quantities in Fig. 1 refer to the stability theory and are explained in the next section.

The dimensionless velocity components in the $x^*$ and $z^*$ directions are the streamwise velocity $U$ and the cross-flow velocity $W$. The reference velocity is $U_p^*$. The reference length is

$$L^* = (\nu_e^* s^* / U_{ce}^*)^{1/2} \tag{1}$$

where $\nu_e^*$ is the kinematic viscosity coefficient evaluated at the edge of the boundary layer, and $s^*$ is the distance along the airfoil surface normal to the leading edge. The Reynolds number is defined as

$$R = U_p^* L^* / \nu_e^* \tag{2}$$

This definition has been chosen because it is nonzero at the leading edge, reduces to the usual boundary-layer Reynolds number for two-dimensional flow, and almost always increases along the wing chord.

Two infinite-span wings are used for the calculations of this paper. One is the 35 deg swept wing with $M_\infty = 0.891$ and chord $c^* = 2.0$ m (measured normal to the leading edge) that has also been analyzed in a number of other papers.[2,6-9] This wing will be referred to as wing A. The other wing is a 23 deg swept wing with $M_\infty = 0.82$ and $c^* = 1.96$ m, and will be referred to as wing L. This wing is to be the subject of an elaborate wind-tunnel test at Langley Research Center (LaRC) and some stability calculations for it have been given by El-Hady.[10]

The pressure coefficient $C_p$ for the upper surface of the 35 deg wing (A) is shown in Fig. 2 as a function of both the chord position ($s^*/c^*$) and the Reynolds number. The value of $R$ at $s^* = 0$ (attachment line) for this wing is 221. The favorable pressure gradient extends to $0.091c^*$ ($R = 1120$) and is followed by a nearly constant, small adverse pressure gradient to $0.31c^*$ ($R = 2060$), and increasing adverse pressure gradient to $0.47c^*$ ($R = 2550$), and then a sharply increasing adverse pressure gradient.

The suction coefficient is defined as

$$C_Q = -\rho_w^* v_w^* / \rho_\infty^* U_\infty^* \tag{3}$$

where $\rho^*$ is the density, $v^*$ is the normal velocity, and $w$ refers to the wall. The distribution of $C_Q$ for which stability calculations have previously been carried out[2,6,8] (called the design suction) is also shown in Fig. 2 along with $W_m$, the corresponding maximum cross-flow velocity, as well as $W_m$ for zero suction. The apparent discontinuity in $W_m$ near $0.4c^*$ is due to the presence of both positive and negative cross flow in the boundary layer in this region. The absolute value of the maximum changes from the negative peak to the positive peak without there being a station where the cross flow is zero. With no suction, laminar separation apparently occurs at about $0.65c^*$ ($R = 3000$). The nonmonotonic behavior of the pressure gradient near $0.55c^*$ ($R = 2750$) is responsible for the "flat spots" in the $W_m$ curves in this region.

The 23 deg wing (L), designed by Dr. W. Pfenninger of LaRC, has an unusual airfoil section with reverse curvature on the lower surface near the leading edge. The upper surface pressure distribution is shown in Fig. 3 and has important differences from wing A. The attachment line Reynolds number of this wing is 155. The nose radius is smaller than for wing A, and the favorable pressure gradient extends only to $0.037c^*$ ($R = 830$). The following adverse pressure gradient is smaller than on wing A and is roughly constant up to about $0.40c^*$ ($R = 2750$). From 0.40 to $0.65c^*$ ($R = 3500$), the pressure gradient is virtually zero. Beyond $0.65c^*$, the adverse pressure gradient increases except for a brief leveling off near $0.77c^*$ ($R = 3800$). The maximum cross-flow velocity for zero suction, $W_{m0}$, is also shown in Fig. 3. Because of the smaller sweep angle, as well as the smaller pressure gradient, the cross flow is much smaller than on wing A over almost all of the chord. Laminar separation with no suction apparently occurs at about $0.75c^*$ ($R = 3750$). An LaRC suction distribution, called the design suction, is shown in Fig. 3 and is intended to maintain full-chord laminar flow. Because this suction does not start until well after the peak cross-flow velocity, it has virtually no effect on the negative cross flow. The main effect is aft of $0.75c^*$ where, in the absence of separation, large, positive cross flow develops.

It should be noted that the usual accuracy and spacing with which the pressure distribution is calculated make it difficult at times to arrive at a reliable value of the pressure gradient for the boundary-layer calculation. The pressure gradient is obtained by numerical differentiation and, where the pressure gradient is small, as on wing A, or changes rapidly, as at some chord locations on both wings, an uneven and unphysical looking distribution of the pressure gradient is obtained. No method of computing the derivative was found that eliminates this problem, and even worse, different methods can give a totally different value of the pressure gradient. The uneven distribution affects the stability calculations, mainly of cross-flow instability, and gave inconsistent looking results at some chord stations. A number of calculations were made with a smoothed pressure gradient and the problem disappeared.

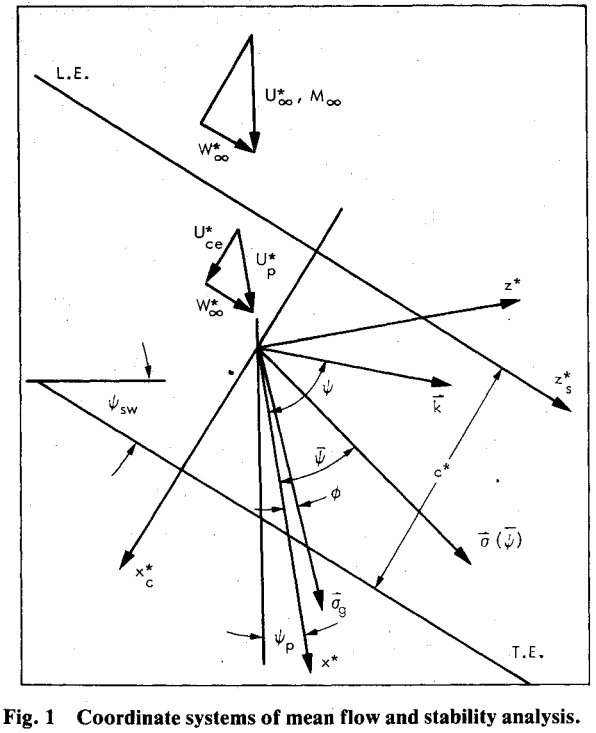


Fig. 1 Coordinate systems of mean flow and stability analysis.

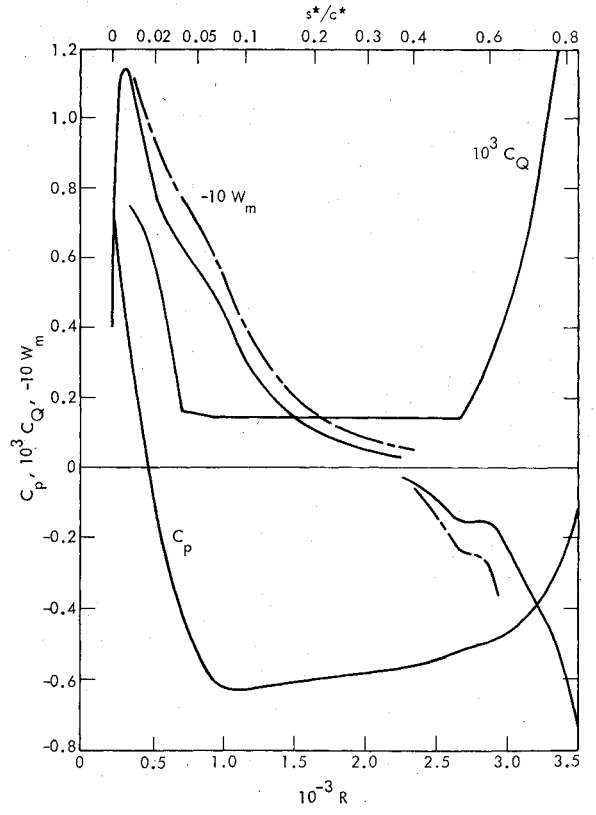


Fig. 2 Pressure coefficient and design suction distribution of 35 deg wing. Maximum cross-flow velocity with design suction ( — ) and without suction ( — - — ).

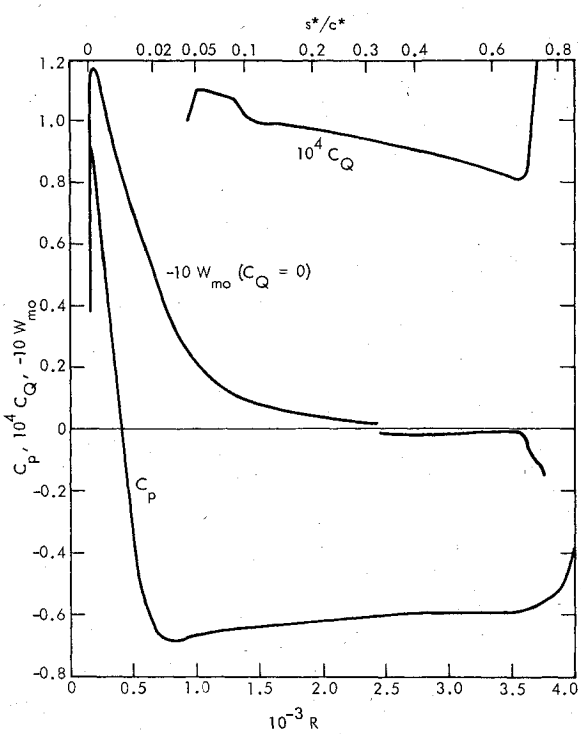


**Fig. 3 Pressure coefficient, design suction distribution, and maximum cross-flow velocity without suction of 23 deg wing.**

However, the smoothing procedure was completely arbitrary, so all stability calculations presented here are for actually computed values of the pressure gradient, using the same method of numerical differentiation, no matter how uneven the results.

## Stability Theory

The computer program used for the calculations is based on the formulation of the three-dimensional stability theory given in Ref. 4. The compressible stability equations are listed in Ref. 6. The sixth-order form of these equations was used because the slight increase in accuracy afforded by the full eighth-order system does not justify the large extra expense its use incurs. The linear stability theory deals with wave components of the form

$$q(x,y,z,t) = A(x,z)\,\zeta(y)\exp[i\theta(x,z,t)] \tag{4}$$

where $q$ is a disturbance flow variable, $A(x,z)$ the amplitude modulation, and $\zeta(y)$ a suitably normalized eigenfunction. All quantities are dimensionless. The complex wavenumber components are

$$\alpha = \partial\theta/\partial x \tag{5a}$$

$$\beta = \partial\theta/\partial z \tag{5b}$$

and the complex frequency is

$$\omega = -\partial\theta/\partial t \tag{5c}$$

The stability equations and the homogeneous boundary conditions constitute an eigenvalue problem whose solution is the complex dispersion relation

$$\omega = \Omega(\alpha,\beta;\, x,z) \tag{6}$$

In the locally parallel-flow theory, $A(x,z)$ is a constant and the spatial amplification rate $(1/q)\mathrm{d}q/\mathrm{d}x$ is independent of both the vertical coordinate $y$ and the particular disturbance quantity $q$. Neither of these statements is true for a nonparallel theory, and the resulting numerical complications make calculation programs such as the one of this paper almost impossible to carry out. Consequently, the traditional approach of evaluating the dispersion relation as if the mean flow velocity components $U(x,y,z)$ and $W(x,y,z)$ were functions of $y$ only will be adhered to. It is to be noted, however, that even with this simplification, the dispersion relation is different at each $x$, $z$ in a growing boundary layer so that $\alpha$, $\beta$, and $\omega$ are functions of $x$ and $z$, and the phase function $\theta(x,z,t)$ cannot be written as $\alpha x+\beta d+\omega t$.

An arbitrary disturbance source will generate a continuum of wave components of the form of Eq. (4), and the observed wave motion will be a superposition of these components. When the source is a localized pulse, this approach has been vigorously pursued by Gaster.[11-13] The simpler and more usual approach is to assume that by the time the wave motion is important for transition, it has evolved to a state such that it is dominated by a single wave component with a real frequency, i.e., a pure spatial wave. Two-dimensional spatial waves are readily produced experimentally in a two-dimensional boundary layer by a vibrating ribbon or other technique. More to the point, in "natural" transition where there is no artificial disturbance source, the observed frequencies are always those of the most amplified spatial wave. However, the experimental evidence[14] is unclear on the question of whether amplification rates measured in natural transition are ever those of a single spatial-wave component. In any case, the use of single spatial waves in transition studies is customary, but there are fundamental questions regarding this approach that remain to be settled.

Even with the restriction to spatial waves computed from the locally parallel theory, there is still one unspecified parameter in the dispersion relation. The frequency $\omega$ is now a real quantity, and the real and imaginary parts of $\alpha$ and $\beta$ can be written separately in polar form as

$$\alpha_r = k\cos\psi \qquad \beta_r = k\sin\psi \tag{7a}$$

$$\alpha_i = -\sigma\cos\bar{\psi} \qquad \beta_i = -\sigma\sin\bar{\psi} \tag{7b}$$

where $k$ and $\psi$ are the magnitude and angle of the wavenumber vector $\boldsymbol{k}$, and $\sigma$ and $\bar{\psi}$ are the magnitude and angle of the spatial amplification rate vector $\boldsymbol{\sigma}$. These angles, as shown in Fig. 1, are defined in the local $x$, $z$ coordinate system where the $x$ axis is aligned with the local potential flow direction. It is the angle $\bar{\psi}$ that must be specified.

Originally, $\bar{\psi}$ was selected on an intuitive basis as the freestream direction for two-dimensional flow and as the group velocity direction for three-dimensional flow. In the ray theory of Gaster for a localized pulse source,[11] $\bar{\psi}$ is set by the condition that the group velocity is real, and in the Cebeci-Stewartson[15] and Nayfeh[16] theories for a localized harmonic source by the condition that the group velocity angle is real. The physical amplification rate $\sigma_g$ is the projection of $\sigma(\bar{\psi})$ in the ray direction $\phi$, where $\phi$ is the (real) group velocity angle and is different from $\bar{\psi}$, except when $\sigma_g$ is a maximum (with respect to $k$). Not only are calculation programs based on the ray theories difficult to carry out, but, as pointed out by Gaster,[17] the above conditions for $\bar{\psi}$ are valid only for a strictly parallel boundary layer and must be replaced by integral saddle-point conditions for a growing boundary layer. Some preliminary calculations for a localized harmonic source in a Blasius boundary layer have shown that the wave amplitudes can be quite different when computed with the Gaster criterion instead of the Cebeci-Stewartson-Nayfeh criterion.

For a two-dimensional boundary layer, or the boundary layer on an infinite-span swept wing, where the boundary layer is independent of $z_s^*$, it is possible to consider a wave motion of uniform amplitude in the $z_s^*$ direction but with variable phase. Such a wave motion, if steady in time, can be well represented as a single spatial oblique wave. Furthermore, in this case the multiple-scale theory of Nayfeh[16]

gives the result that the complex spanwise wavenumber component is independent of $x_c^*$, which is a generalization of the conservative wave-theory relation $\nabla \times \boldsymbol{k} = 0$ to the nonconservative case, where $\boldsymbol{k}$ is replaced by a complex vector. The real form of this relation has been used previously in two-dimensional boundary-layer stability calculations,[4] and the complex form adds a condition on $\bar{\psi}$. The initial $\bar{\psi}$ is still unspecified, but it is in accord with the assumed wave motion to take $\bar{\psi}=0$ for a two-dimensional boundary layer, and $\bar{\psi}=-\psi_p-\psi_{sw}$ for the infinite swept-wing boundary layer. In both cases, $\sigma(\bar{\psi})$ is also the physical amplification rate.

The amplification rates in the next section have all been computed with $\bar{\psi}=0$ in order to be consistent with the previous calculations of this series. The chordwise amplification rate for this value of $\bar{\psi}$ is, of course, simply $\sigma\cos(\psi_p+\psi_{sw})$. However, the physical amplification rate $\sigma_c$, as defined in the preceding paragraph for an oblique wave, requires the eigenvalues to be computed with $\bar{\psi}=-\psi_p-\psi_{sw}$. This amplification rate is related to $\sigma_g$, the amplification rate with $\bar{\psi}=\phi$, with good accuracy by $\sigma_c=\sigma_g/\cos(\psi_p+\psi_{sw}+\phi)$.[4] The more exact transformation of Nayfeh and Padhye[18] reduces to this relation when the group velocity angle is real. In turn, $\sigma$ (with $\bar{\psi}=0$ deg) is related to $\sigma_g$ by $\sigma=\sigma_g/\cos\phi$. As $\phi$ is only a few degrees at most, $\sigma\cong\sigma_g$ and $\sigma_c$ can be obtained from $\sigma$ provided $\phi$ is known. Even if $\phi$ is not known, $\sigma_c$ can still be estimated. Except very close to the leading edge, $\psi_p$ is almost constant at $-8.5$ deg for wing A, and at $-5.5$ deg for wing B. Consequently, $\sigma_c$ is given within about 5% for both wings simply by setting $\phi=0$ deg in the cosine relation. For the type of calculations given in this paper, either $\sigma$ or $\sigma_c$, or any consistently defined amplification rate, is suitable. It is only when the wave amplitude is to be computed that the proper amplification rate for the assumed wave motion is required.

The dimensionless frequency which appears in the stability results is defined as

$$F=\omega^* \nu_\infty^* / U_\infty^{*2} \tag{8}$$

where $\omega/r^*$ is the circular frequency. This is the usual definition of $F$, but with reference conditions in the undisturbed freestream rather than the edge of the boundary layer so that a constant $F$ is the same as a constant dimensional frequency. The maximum amplification rate is referenced to $L^*$ as given by Eq. (1).

The maximum amplification rate of the stationary disturbances was found by calculating $\sigma$ with $\bar{\psi}=0$ deg at five values of the wavenumber $k$, making a least-squares fit to the results and computing the maximum from the analytic approximating function. For the $\psi=0$ deg waves, the maximum is with respect to frequency. At least five frequencies were used to locate the maximum, although usually the program was allowed to cover the entire unstable frequency range in order to locate the frequencies of neutral stability. As mentioned in the Introduction, this investigation is restricted to waves of maximum amplification rate with $F=0$ or $\psi=0$ deg for the purpose of keeping the number of calculations within a reasonable limit. Coincidentally, the ray condition of real group velocity angle is very nearly satisfied for the $F=0$ waves, but not for the $\psi=0$ deg waves. However, it is not being suggested, as for example in Ref. 10, that this ray condition restricts stationary waves to waves of maximum amplification rate. The adjustable parameter to satisfy the ray condition is $\bar{\psi}$, and it is only exceptionally that $\bar{\psi}=\phi$ and $\sigma_g$ is a maximum with respect to $k$.

## Numerical Results

Detailed results for wing A (35 deg) with the design suction distribution of Fig. 2 have been given previously.[6,8] The results given here for this wing are included mainly to contrast with those of wing L (23 deg), which is the main subject of this paper. The distribution of the maximum spatial amplification rate $\sigma_m$ along the wing chord for wing A without suction is shown in Fig. 4 for the stationary ($F=0$) and $\psi=0$ deg disturbances. For $F=0$, the maximum is with respect to the wavenumber $k$; for $\psi=0$ deg, it is with respect to the frequency $F$. The distribution of $\sigma_m$ for $F=0$ is somewhat similar to that of the maximum cross-flow velocity $W_m$, as was also found with the design suction in Ref. 6. Although the cross flow on this wing without suction is sufficient to maintain unstable stationary disturbances at all chord stations greater than $0.003c^*$, the two $F=0$ curves for positive and negative cross flow are not connected in Fig. 4 in order to emphasize that when the cross flow reverses, the orientation of $k$ changes by about 180 deg. Consequently, the disturbances in the positive cross-flow region are unrelated to those in the negative cross-flow region.

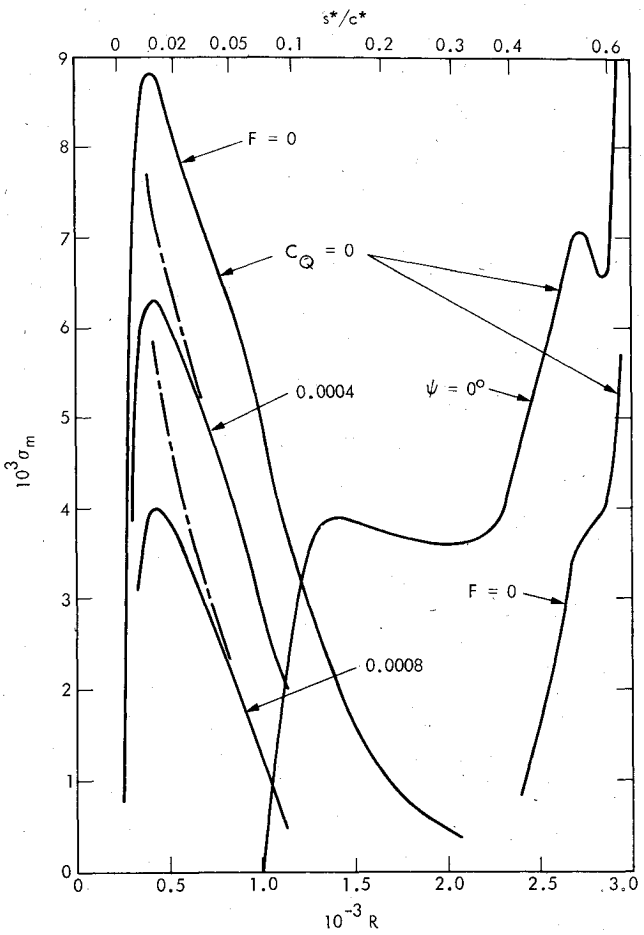


**Fig. 4 Maximum spatial amplification rate of stationary ($F=0$) and traveling-wave ($\psi=0$ deg) disturbances for 35 deg wing without suction, and of stationary disturbances with $C_Q=0.0004$ and 0.0008 starting at leading edge ( — ) and at $0.009c^*$ ( — — — ).**

The traveling-wave disturbances are not dependent on the cross flow for their existence, but are modified by it. The first computed chord station where the $\psi=0$ deg waves are unstable is $0.094c^*$ ($R=1131$). This is also the first station with a generalized inflection point† in the streamwise boundary-layer profile. Thus, the streamwise profile is much more sensitive to the local pressure gradient than is the cross-flow profile, and this sensitivity shows up immediately in the streamwise instability. The local cross flow, and hence cross-flow instability, depends very much on the upstream boundary layer. For example, the cross flow does not reverse until far downstream from the start of the adverse pressure gradient, as seen in Fig. 2.

†A generalized inflection point is where $(U'/T')'=0$ [$T$ is the temperature and $(\,)'$ is d/d$y$], and is the condition for compressible inviscid instability.

The almost flat portion of the $\sigma_m$ curve for $\psi = 0$ deg waves in Fig. 4 is due to the nearly constant pressure gradient, with the generalized inflection point remaining at almost the same $y/\delta$ ($\delta$ is the boundary-layer thickness). The steep rise in $\sigma_m$ near $0.35c^*$ ($R = 2200$) results from an increase in the adverse pressure gradient and the outward movement of the generalized inflection point. The nonmonotonic behavior of $\sigma_m$ near $0.55c^*$ ($R = 2750$) is caused by an unevenness in the pressure gradient in that region. As the boundary layer thickens in the strong adverse pressure gradient just before laminar separation (at about $0.65c^*$, $R = 3000$), there is a precipitous rise in the amplification rates of both types of disturbances.

Figure 4 also gives $\sigma_m$ for stationary disturbances with $C_Q = 0.0004$ and 0.0008 starting at the leading edge. It will be seen by comparison with the design suction distribution of Fig. 2 that these are much larger suction magnitudes than believed necessary to maintain laminar flow, but even so, do not come close to completely stabilizing the boundary layer in the region where the cross-flow velocity without suction is greater than 5%. Also shown for these two suction magnitudes is the effect of delaying the start of the suction until $0.009c^*$ ($R = 355$), where the design suction starts. The amplification rates eventually become the same as with suction from the leading edge, with the adjustment distance being longer for the larger suction rate.

The distribution along the chord of $\sigma_m$ for the $F = 0$ and $\psi = 0$ deg disturbances of wing L (23 deg) with both the design suction of Fig. 3 and without suction is shown in Fig. 5. There is a marked difference between the cross-flow instability on this wing and on wing A. Because of the reduced cross flow on wing L, the stationary disturbances without suction have, at most, only about the same amplification rate as with $C_Q = 0.0008$ for wing A. Consequently, suction is only needed to control the traveling waves, except in the rear of the wing. The design suction does not start until $0.04c^*$ ($R = 858$) and, as seen in Fig. 5, has virtually no effect on the stationary disturbances.

Without suction, the $\psi = 0$ deg waves have about the same maximum amplification rate in the small adverse pressure gradient region between $0.05c^*$ ($R = 970$) and $0.65c^*$ ($R = 3500$) as in the similar region of wing A between $0.10c^*$ ($R = 1150$) and $0.35c^*$ ($R = 2200$), where, however, the pressure gradient is larger. The design suction of wing L up to $0.75c^*$ ($R = 3760$) is only 60-70% of what it is on wing A where the $\psi = 0$ deg waves are almost completely stabilized, but it still effectively controls the instability of these waves in this region as is shown in Fig. 5 by the large decrease in $\sigma_m$ with suction. It must be recalled that the frequency of each $\sigma_m$ in Fig. 5 is different (see Fig. 6), so that $\psi = 0$ deg waves of a given frequency have a much smaller amplitude growth than a fictitious wave amplifying with $\sigma_m$ everywhere.

Between $0.35c^*$ ($R = 2200$) and $0.60c^*$ ($R = 3340$), where the pressure gradient is almost zero, the instability closely resembles that of a flat-plate boundary layer. The cross flow is too small for cross-flow instability, and the most unstable traveling waves are oblique with only a slight asymmetry to betray the existence of a small cross flow. For example, at $0.15c^*$ ($R = 1700$), where $W_m = -0.006$, the wave angles of the most unstable waves are $-48$ and 41 deg, with $\sigma_m \times 10^3 = 4.93$ and 4.44, respectively. For the $\psi = 0$ deg wave, $\sigma_m \times 10^3 = 4.00$. For all three waves, $F_m = 0.21 \times 10^{-4}$. At $0.60c^*$ ($R = 3390$), where $W_m = 0.0008$, the most unstable wave angles are $-49$ and 48 deg, and $\sigma_m \times 10^3 = 3.92$ and 3.83, respectively. Here, $\sigma_m \times 10^3 = 3.15$ for the $\psi = 0$ deg wave, and $F_m = 0.07 \times 10^{-4}$ for all three waves.

At about $0.65c^*$ ($R = 3500$), the adverse pressure gradient starts to increase rapidly, and the distribution of $\sigma_m$ with $\psi$ becomes quite unlike what it is in a two-dimensional boundary layer. The maximum amplification rate of the $\psi = 0$ deg waves increases rapidly as shown in Fig. 5, and a sharp increase in suction (Fig. 3) is required to control this instability. However, even with this large suction, cross-flow instability reappears and $\sigma_m$ of the stationary disturbances becomes very large at Reynolds numbers larger than shown in Fig. 5.

The neutral-stability curve of frequency vs Reynolds number for the $\psi = 0$ deg waves of wing A without suction is shown in Fig. 6 along with the most unstable frequency. The appearance of the neutral curve resembles those of two-dimensional, self-similar boundary layers up to about $0.61c^*$ ($R = 3400$). The unstable frequency band shifts to lower frequencies with increasing $s^*$, and the distance over which a given frequency is unstable increases. The ratio of the upper-branch frequency to the lower-branch frequency is about 4:1. Between $0.61c^*$ and laminar separation, along with the precipitous rise in the amplification rate shown in Fig. 5, there is both an increase in the upper-branch frequency and a large increase in the ratio of the upper-branch frequency to the lower-branch frequency from 4:1 to 30:1. The wide unstable

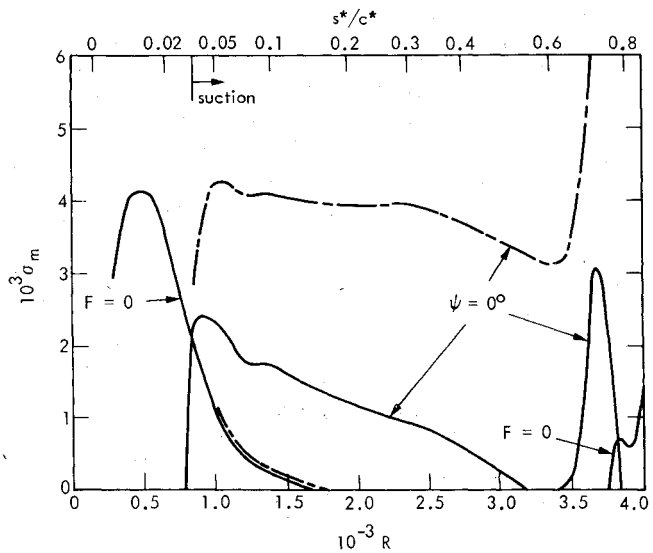


**Fig. 5 Maximum spatial amplification rate of stationary ($F = 0$) and traveling-wave ($\psi = 0$ deg) disturbances for 23 deg wing with design suction ( — ) and without suction ( — - — ).**

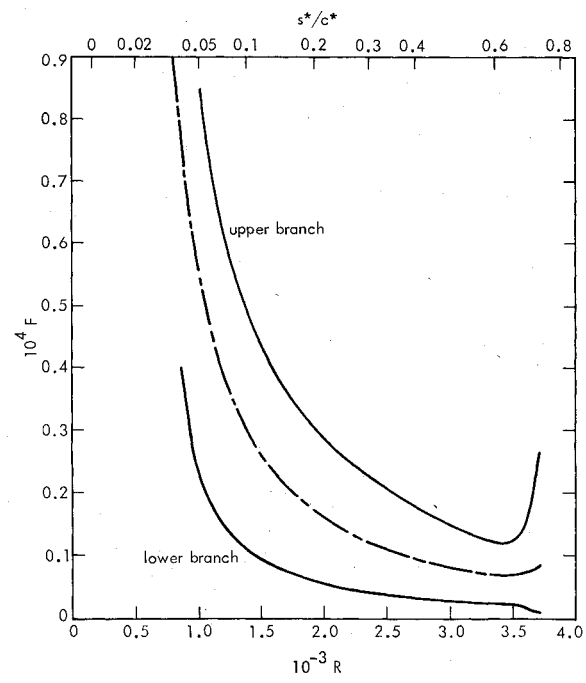


**Fig. 6 Neutral-stability boundaries ( — ) and most unstable frequencies ( — - — ) of $\psi = 0$ deg traveling-wave disturbances for 23 deg wing.**

frequency band combined with high amplification rates is characteristic of boundary layers with a large adverse pressure gradient, and is found also in the Falkner-Skan family near separation.

Suction reduces cross-flow instability by reducing the amount of cross flow. Figure 7 shows the fractional decrease in the maximum cross-flow velocity $\Delta W_m/W_{m0}$ ($W_{m0}$ is $W_m$ for zero suction and $\Delta W_m = W_{m0} - W_m$) as a function of the similarity suction parameter $-\rho_w v_w R$ ($w$ refers to the wall, $\rho$ is referenced to the density at the boundary-layer edge, and $v$ to $U_p^*$) at three chord stations in the negative cross-flow region of wing L. The suction mass flux is uniform from the leading edge.

For a given self-similar boundary layer with a similarity suction distribution, $\Delta W_m/W_{m0}$ depends only on the suction parameter and is independent of the amount of cross flow (which depends on $\psi_p + \psi_{sw}$).[7] As seen in Fig. 7, even for the nonsimilar boundary layer of wing L with a constant suction distribution, the cross-flow reductions at various stations have a tendency to fall together when plotted as a function of this parameter. The three stations of Fig. 7 are $0.005c^*$ ($R=271$), where $W_{m0}$ has its peak value of $-0.118$; $0.0175c^*$ ($R=572$), where $W_{m0}=-0.062$; and $0.103c^*$ ($R=1393$), where $W_{m0}=-0.0096$. Also shown by the broken curve is the variation of $\Delta W_m/W_{m0}$ between $0.005c^*$ and $0.103c^*$ for the fixed suction $C_Q=0.0008$.

The fractional reduction in the maximum amplification rate of the stationary disturbances of wing L that accompanies the cross-flow reduction of Fig. 7 is given in Fig. 8. The ratio $\Delta\sigma_m/\sigma_{m0}$ ($\sigma_{m0}$ is $\sigma_m$ with zero suction, and $\Delta\sigma_m = \sigma_{m0} - \sigma_m$) is plotted against $C_Q$ itself because there is little apparent tendency for $\Delta\sigma_m/\sigma_{m0}$ to scale in terms of $-\rho_w v_w R$. It can be seen that the fractional reduction is close to being a linear function of $C_Q$ up to at least a reduction of about 50%, and that for the final station at $0.103c^*$, it is linear all the way to complete stabilization.

At first, the stabilization decreases with increasing $s^*$ and a fixed $C_Q$. Indeed, the curve for $0.005c^*$ (not shown) is, by chance, almost coincident with that for $0.054c^*$ (labeled as $0.05c^*$) shown in Fig. 8. However, from $0.017c^*$, the stabilization increases with increasing $s^*$. This latter behavior is to some extent merely a reflection of what would seem evident, that the smaller the cross flow the less suction is required for complete stabilization. However, the similarity solutions of Ref. 7 showed that $\Delta\sigma_m/\sigma_{m0}$ is also a function of both Reynolds number and the pressure gradient. These two factors are also important for swept-wing boundary layers, as evidenced by the same suction resulting in less stabilization when the cross flow is less for $s^* < 0.017c^*$, but more computations are needed to sort out the individual influences of the pressure gradient, Reynolds number, and cross flow.

Figure 9 is equivalent to Fig. 8, but is for the $\psi=0$ deg traveling-wave disturbances on wing L instead of the stationary disturbances. Again, $\Delta\sigma_m/\sigma_{m0}$ is initially a linear function of $C_Q$, but here the linear range extends to a fractional reduction in the maximum amplification rate of about 70%. Six chord stations are shown in Fig. 9, and at $0.63c^*$ the curve is continued past complete stabilization into the damped region. One prominent feature of Fig. 9 is the difference in the $C_Q$ scale compared to Fig. 8. As is true of all waves of the Tollmien-Schlichting type, the $\psi=0$ deg waves are more readily stabilized by suction than are the stationary waves. This same result was found previously for incompressible Falkner-Skan-Cooke boundary layers.[7]

The slopes of the curves in Fig. 9 have a more complex variation with chord position than in Fig. 8. Starting at the smallest $s^*$ of $0.04c^*$, the stabilization for a fixed $C_Q$ decreases with increasing $s^*$ to $0.05c^*$, then increases up to $0.63c^*$, followed by another decrease to $0.72c^*$ which is just before laminar separation. Nothing is known about the reasons for these changes, but to arrive at a greater understanding, it will probably be necessary to examine traveling-wave instability more completely and not just depend on the representation by the $\psi=0$ deg waves.

The effect of the suction starting location on $\psi=0$ deg waves was investigated by means of three constant mass flux distributions starting at $0.039c^*$ ($R=858$), where the design suction also starts. Somewhat surprisingly, the delayed start was found to have virtually no effect except at the initial suction station itself. By the next station ($0.046c^*$, $R=934$), the difference in $\sigma_m$ produced by the delayed start is only

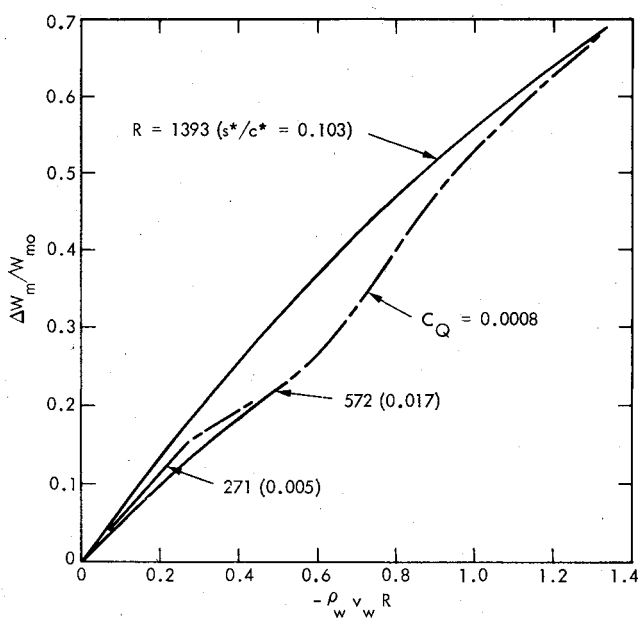


**Fig. 7 Fractional reduction in maximum cross-flow velocity as function of similarity suction parameter in negative cross-flow region of 23 deg wing with constant suction mass flux starting at leading edge.**

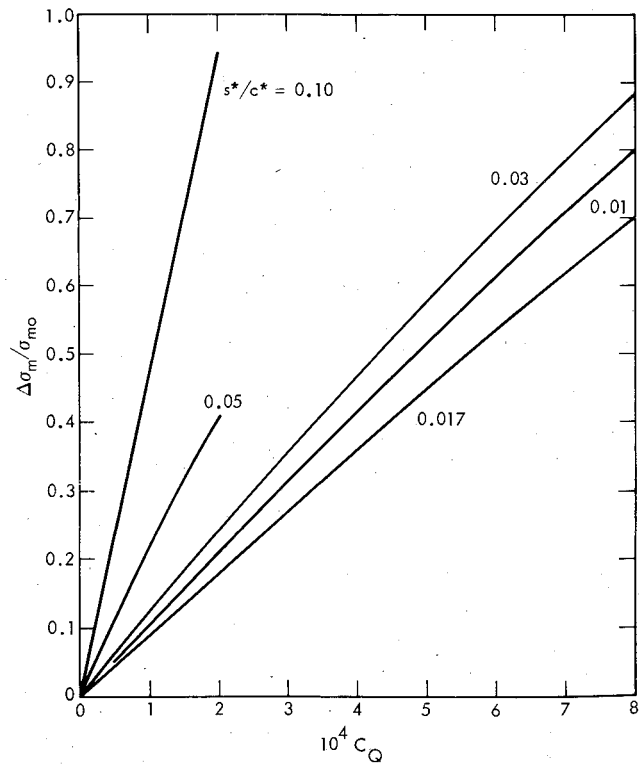


**Fig. 8 Fractional reduction in maximum spatial amplification rate of stationary disturbances ($F=0$) at five chord stations in negative cross-flow region of 23 deg wing. Constant suction mass flux starting at leading edge.**

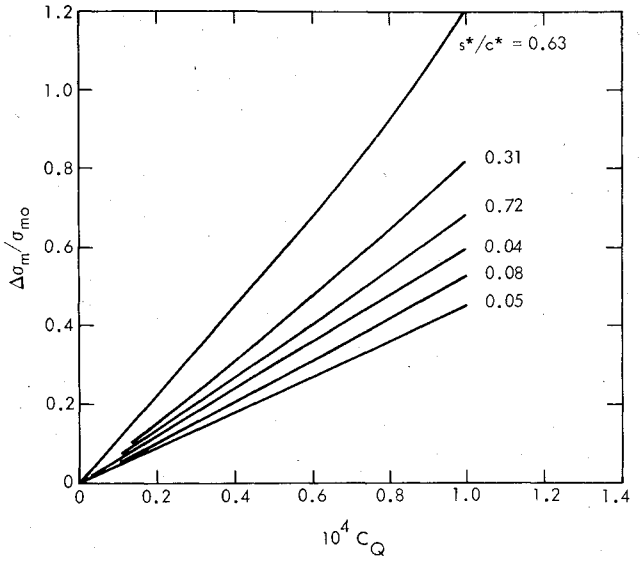


**Fig. 9 Fractional reduction in maximum spatial amplification rate of traveling-wave disturbances ($\psi = 0$ deg) at six chord stations of 23 deg wing. Constant suction mass flux starting at leading edge.**

2.6%, and at $0.082c^*$ there is no longer any difference at all. This lack of influence of the suction starting point is one reason why $\Delta\sigma_m/\sigma_{m0}$ for the design suction is very close to the curves of Fig. 9, except near the starting point and in the region to the rear of the wing where $C_Q$ changes rapidly.

## Concluding Remarks

The study of the 35 and 23 deg wings has given a reasonably complete view of the most important features of the linear instability of swept-wing boundary layers, and has demonstrated how the instability is influenced by pressure gradient and suction. The near linearity of the maximum amplification rates of both stationary and $\psi = 0$ deg disturbances with the suction magnitude, which for the latter disturbances is true even when the suction is slowly varying along the chord, can help reduce the amount of computation needed to arrive at a design suction distribution for laminar flow control.

It must be emphasized that the instability of a three-dimensional boundary layer is much more complicated than for a two-dimensional boundary layer, and that the expedient of examining it by means of $F = 0$ and $\psi = 0$ deg waves alone is a drastic, and not entirely satisfactory, simplification. When cross-flow instability is dominant, as near the leading edge, the stationary waves seem to always have a $\sigma_m$ within about 20% of the largest possible amplification rate and are a good representation of this instability. But even here, as the complete stability diagrams of Ref. 5 have shown, there are unstable disturbances covering a wide band of frequencies and wavenumbers.

When more than cross-flow instability is present, the full complications have not yet been worked out, although a few examples may be found in Refs. 5 and 6. Particularly when a large, or even moderate, adverse pressure gradient is combined with cross flow, which need not be large, the distinction between cross-flow and streamwise instability is not at all clear, and both the $F = 0$ and $\psi = 0$ deg waves can be of minor importance compared to other waves with much larger amplification rates. Many of these instabilities change rapidly along the chord, so it may not be possible for them to build up appreciable amplitudes, but it is well to keep in mind that a wide variety of unstable waves of many frequencies, wavenumbers, and orientations exist in a three-dimensional boundary layer. Some of these other waves, rather than the most obvious candidates, especially when the latter have been selected by physically unrealistic calculation methods, may also be obstacles preventing the maintenance of the desired laminar flow.

## Acknowledgment

This paper represents the result of research carried out at the Jet Propulsion Laboratory, California Institute of Technology, under NASA Contract NAS7-100. The work on the 23 deg swept wing was supported by the NASA Langley Research Center.

## References

[1] Brown, W. B., "A Stability Criterion for Three-Dimensional Laminar Boundary Layers," *Boundary Layer and Flow Control,* Vol. 2, Pergamon Press, New York, 1961, pp. 913-923.

[2] Srokowski, A. J. and Orszag, S. A., "Mass Flow Requirements for LFC Wing Design," AIAA Paper 77-1222, Aug. 1977.

[3] Hefner, J. N. and Bushnell, D. M., "Application of Stability Theory to Laminar Flow Control," AIAA Paper 79-1493, July 1979.

[4] Mack, L. M., "Transition Prediction and Linear Stability Theory," *Laminar-Turbulent Transition,* AGARD Conference Proceedings No. 224, Oct. 1977, pp. 1-13-1-22.

[5] Mack, L. M., "Three-Dimensional Effects in Boundary-Layer Stability," *Twelfth Symposium on Naval Hydrodynamics,* National Academy of Sciences, Washington, D. C., 1979, pp. 63-76.

[6] Mack, L. M., "On the Stability of the Boundary Layer on a Transonic Swept Wing," AIAA Paper 79-0264, Jan. 1979.

[7] Mack, L. M., "On the Stabilization of Laminar Boundary Layers by Suction and Cooling," *Proceedings of IUTAM Symposium on Laminar-Turbulent Transition,* Springer-Verlag, Berlin, 1980, pp. 223-238.

[8] Lekoudis, S., "Stability of Three-Dimensional Compressible Boundary Layers over Wings with Suction," AIAA Paper 79-0265, Jan. 1979.

[9] Lekoudis, S., "Stability of the Boundary Layer on a Swept Wing with Wall Cooling," *AIAA Journal,* Vol. 18, Sept. 1980, pp. 1029-1035.

[10] El-Hady, N. M., "On the Stability of Three-Dimensional Compressible Nonparallel Boundary Layers," AIAA Paper 80-1374, July 1980.

[11] Gaster, M., "The Development of Three-Dimensional Wave Packets in a Boundary Layer," *Journal of Fluid Mechanics,* Vol. 32, Pt. 1, 1968, pp. 173-184.

[12] Gaster, M., "A Theoretical Model of a Wave Packet in the Boundary Layer on a Flat Plate," *Proceedings of the Royal Society of London,* Series A, Vol. 347, 1975, pp. 271-289.

[13] Gaster, M., "The Propagation of Linear Wave Packets in Laminar Boundary Layers," *AIAA Journal,* Vol. 19, April 1981, pp. 419-423.

[14] Kendall, J. M., "Wind Tunnel Experiments Relating to Supersonic and Hypersonic Boundary-Layer Transition," *AIAA Journal,* Vol. 13, March 1975, pp. 290-299.

[15] Cebeci, T. and Stewartson, K., "On Stability and Transition in Three-Dimensional Flows," *AIAA Journal,* Vol. 18, April 1980, pp. 398-405.

[16] Nayfeh, A. H., "Stability of Three-Dimensional Boundary Layers," *AIAA Journal,* Vol. 18, April 1980, pp. 406-416.

[17] Gaster, M., "The Development of a Wave Packet in a Growing Boundary Layer" (unpublished), 1979.

[18] Nayfeh, A. H. and Padhye, A., "The Relation between Temporal and Spatial Stability in Three-Dimensional Flows," *AIAA Journal,* Vol. 17, Oct. 1979, pp. 1084-1090.